Analysis of a wavelength selectable cascaded DFB laser based on the transfer matrix method*

Xie Hongyun(谢红云)†, Chen Liang(陈亮), Shen Pei(沈珮), Sun Botao(孙博韬), Wang Renqing(王任卿), Xiao Ying(肖盈), You Yunxia(尤云霞), and Zhang Wanrong(张万荣)

(College of Electronic Information and Control Engineering, Beijing University of Technology, Beijing 100124, China)

Abstract: A novel cascaded DFB laser, which consists of two serial gratings to provide selectable wavelengths, is presented and analyzed by the transfer matrix method. In this method, efficient facet reflectivity is derived from the transfer matrix built for each serial section and is then used to simulate the performance of the novel cascaded DFB laser through self-consistently solving the gain equation, the coupled wave equation and the current continuity equations. The simulations prove the feasibility of this kind of wavelength selectable laser and a corresponding designed device with two selectable wavelengths of 1.51 μm and 1.53 μm is realized by experiments on InP-based multiple quantum well structure.

Key words: transfer matrix method; cascaded DFB laser; selectable wavelengths
DOI: 10.1088/1674-4926/31/6/064006 **PACC:** 4255P; 4260D; 4280S

1. Introduction

Several modern communication systems, such as metro networks, access networks and fiber to the home systems (FTTH), all favor coarse wavelength division multiplexing (CWDM) to avoid the high cost and system complexity of dense wavelength division multiplexing (DWDM). CWDM spans the S-band, C-band and L-band (1270–1610 nm) with a wavelength spacing of 20 nm (ITU-T G694.2) and initially gives its devices low cost and simplicity[1]. But state-of-the-art transmitters are still complex and high-cost modules consisting of independent parallel DFB lasers. As an effective solution, fabricating a transmitter with monolithic integration technology can make the process simpler[2] and lower cost.

In this paper, a new monolithically integrated device including two serial Bragg gratings is designed and analyzed with the transfer matrix method (TMM). To simulate the device performance, two cascade sections are analyzed separately through the efficient facet reflectivity derived from each transfer matrix. Both the simulation results and measurements prove this monolithically integrated device can provide two electable wavelengths with a space of 20 nm.

2. Device design

2.1. Device structure

A cascaded DFB laser is proposed to avoid large transmission loss produced by a multiple mode interferometer (MMI) which is a necessary component in the light source module used in CWDM[3, 4]. Figure 1 illustrates the cascaded structure. In sections P1 and P2, two different Bragg gratings are fabricated separately to provide two Bragg wavelengths with a spacing of 20 nm. The grating with short period is fabricated in the front section P1, and the other grating with longer period is fabricated in the rear section P2. A short wavelength laser emits from the left facet directly, a longer wavelength laser transmits through P1 and emits from the left facet too. The photon energy of the longer wavelength laser is lower than the energy required to stimulate the short wavelength laser in P1, so it is possible that the longer wavelength laser transmits through P1 without inducing lasing action in it. Moreover, the spacing of 20 nm is large enough to neglect the interaction between these two gratings. Therefore, this device structure can ensure excellent single-mode performance and almost equal light power level of the two wavelengths[5]. Here, the Bragg wavelength of the front section P1 is chosen as 1.51 μm and that of the rear section P2 is chosen as 1.53 μm.

2.2. Device model

There are two active sections in this cascaded device. It would be a little more complex to analyze its performance

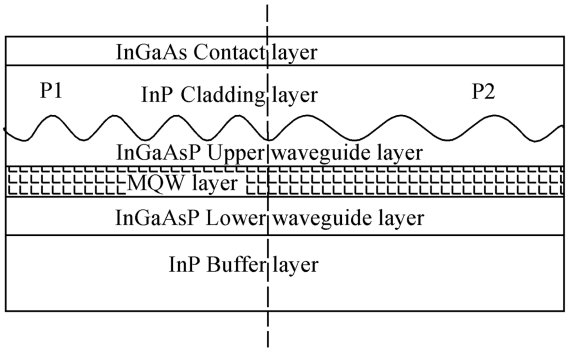

Fig. 1. Sketch of cascaded DFB laser.

* Project supported by the National Natural Science Foundation of China (Nos. 60776051, 60376033), the Beijing Municipal Natural Science Foundation of China (No. 4082007), and the Beijing Municipal Education Committee of China (Nos. KM200910005001, KM200710005015).

† Corresponding author. Email: xiehongyun@bjut.edu.cn

Received 23 November 2009, revised manuscript received 1 February 2010 © 2010 Chinese Institute of Electronics

directly through the beam propagation method (BPM), so a novel device model based on efficient facet reflectivity derived through TMM is explored to analyze these two sections separately.

The transfer matrix of the left facet or right facet is given in Eq. (1):

$$F_{\text{left/right}}(r) = \begin{bmatrix} 1/(1-r) & -r/(1-r) \\ -r/(1-r) & 1/(1-r) \end{bmatrix}, \tag{1}$$

where r is the facet field reflectivity of InP-based material (usually 0.57).

The transfer matrix of P1 or P2 is given in Eq. (2) considering the sinusoidal Bragg grating in it:

$$F_{\text{P1/P2}} = \begin{bmatrix} \cosh(qL) - \dfrac{\mathrm{i}(\Delta\beta + \mathrm{i}g)}{q}\sinh(qL) & -\dfrac{\mathrm{i}\kappa}{q}\sinh(qL) \\ \dfrac{\mathrm{i}\kappa}{q}\sinh(qL) & \cosh(qL) + \dfrac{\mathrm{i}(\Delta\beta + \mathrm{i}g)}{q}\sinh(qL) \end{bmatrix}, \tag{2}$$

where g is the gain of the active area and depends on the facet power reflectivity as $2gL = \ln(1/R)$, $\Delta\beta$ is the deviation between the propagation constant β and the Bragg propagation constant β_{B} and $\Delta\beta = \beta - \beta_{\text{B}} = \frac{2\pi n_{\text{eff}}(\lambda)}{\lambda} - \frac{2\pi n_{\text{eff}}(\lambda_{\text{B}})}{\lambda_{\text{B}}} \approx \frac{2\pi n_{\text{g}}}{\lambda_{\text{B}}^2}\Delta\lambda$. κ is the coupling coefficient and $q^2 = \kappa^2 - (\Delta\beta + \mathrm{i}g)^2$.

P1 is considered as a common DFB laser. Its front facet is the cleavage plane and its rear facet is an equivalent reflective plane of the section P2 and the actual rear facet. The equivalent rear field reflectivity is derived from Eq. (3):

$$r_{\text{equr-21}} = -\frac{(F_{\text{equ-rear}})_{21}}{(F_{\text{equ-rear}})_{22}}, \tag{3}$$

where $F_{\text{equ-rear}}$ is expressed as Eq. (4), which is the equivalent transfer matrix of the rear section P2 and the actual rear facet:

$$F_{\text{equ-rear}} = F_{\text{P2}} F_{\text{right}}(r). \tag{4}$$

After calculation, the equivalent rear field reflectivity of the front DFB laser $r_{\text{equr-21}}$ is 0.63. Then the equivalent rear facet power reflectivity of it, $R_{\text{equr-21}}$, is 0.397.

P2 is analyzed in the same way through analyzing Eqs. (5) and (6).

$$r_{\text{equf-21}} = -\frac{(F_{\text{equ-front}})_{21}}{(F_{\text{equ-front}})_{22}}, \tag{5}$$

$$F_{\text{equ-front}} = F_{\text{P1}} F_{\text{left}}(r). \tag{6}$$

Correspondingly, the equivalent front field reflectivity of the rear DFB laser $r_{\text{equf-21}}$ is 0.553 and the equivalent front facet power reflectivity of it, $R_{\text{equf-21}}$, is 0.306.

The parameters used in the calculation are given in Table 1.

A sketch of a common DFB laser used in simulation is illustrated in Fig. 2.

At first, through solving the Schrödinger equation (7) based on the perturbation theory of $k \cdot \hat{p}$, the energy distribution in the quantum well structure is achieved and given in Eq. (8). The material gain spectrum is derived from the obtained energy distribution.

$$[H_0 + V(r)]\psi(r) = E(r)\psi(r), \tag{7}$$

$$E(n_z, k_x, k_y) = \frac{\hbar^2}{2m^*}(k_x^2 + k_y^2) + E_{zn},$$

$$\frac{L\sqrt{2m^* E_{zn}}}{\hbar} = \arctan\sqrt{\frac{V_0 - E_{zn}}{E_i}} + n\pi, \quad n_z = 1, 2, 3, \cdots. \tag{8}$$

A photon beam propagates along the z-direction in the waveguide structure. The wave equation is presented in Eq. (9). With the technique of variable separation, it is solved as Eq. (10):

$$\frac{\partial^2}{\partial x^2 y^2}E(x, y, z) + \frac{\partial^2}{\partial z^2}E(x, y, z) + k_0^2[n_{\text{eff}} + \Delta n(x, y, z)]^2 E(x, y, z) = 0, \tag{9}$$

$$E(x, y, z) = E(z)\phi_0(x, y). \tag{10}$$

Usually, the DFB laser is assumed to operate at a single transverse mode. The exact transverse mode distribution $\phi_0(x, y)$ is calculated effectively by the effective index method. The z-dependent part of the electric field satisfies Eq. (11):

$$\left[\frac{\partial^2}{\partial z^2} + k_0^2 n(z)^2\right] E(z) = f(z), \tag{11}$$

where $f(z)$ is the Langevin noise function due to spontaneous emission, the complex propagation constant $t(z)$ is calculated from the effective index at a specific cross section in the xy-plane.

For the DFB laser, the coupling between forward and backward waves must be considered into the effective refractive index along the waveguide structure. So Equation (11) evolves into the coupled wave equation (12)[6]. It can be solved conveniently with the transfer matrix method.

$$\frac{\mathrm{d}}{\mathrm{d}z}r(z) = -\mathrm{i}\Delta\beta r(z) - \mathrm{i}\kappa s(z),$$

$$\frac{\mathrm{d}}{\mathrm{d}z}s(z) = \mathrm{i}\Delta\beta s(z) + \mathrm{i}\kappa r(z). \tag{12}$$

Equation (13) is the current continuity equation, the general relation between the injection current, the photon density and the carrier densities involving the mechanisms of stimulated recombination and various other recombination terms, drift and diffusion contributions.

$$F_{\text{rate}}(z, J, S, N) = 0. \tag{13}$$

Table 1. Parameters used in simulation of the serial DFB laser.

Parameter	Value	Parameter	Value
n_g	4	n_1	3.286
λ_B	1.51 μm/1.53 μm	n_2	3.167
$\Delta\lambda$	–20/20 nm	L	300 μm
d_g	80 nn	R	0.32

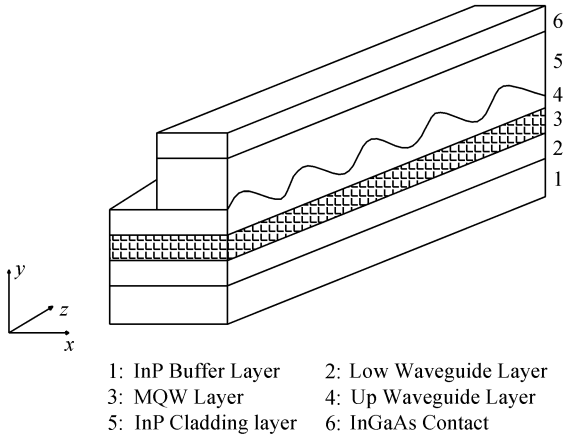

Fig. 2. Sketch of a DFB laser for simulation.

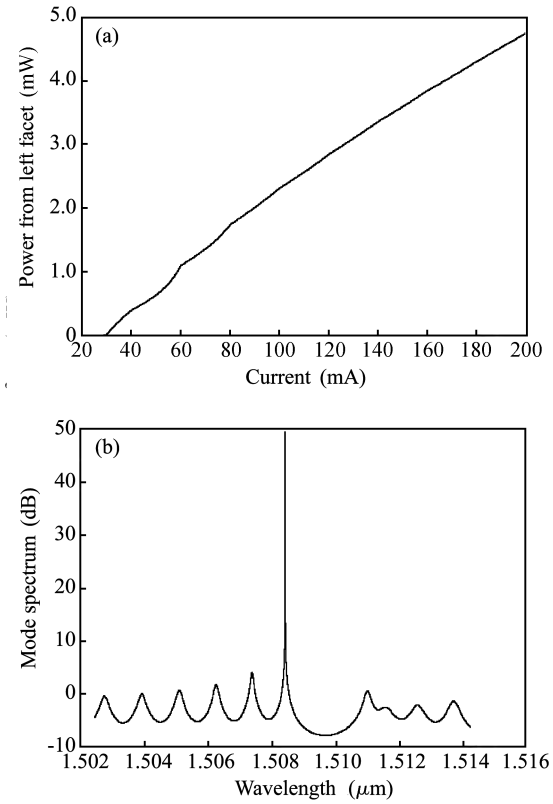

Fig. 3. Simulation results of (a) P–I curve and (b) spectrum of the front DFB section.

With a proper starting injected current, the gain equation, the coupled wave equation and the current continuity equation are self-consistently solved by the Newton iteration method. A fine mesh grid is used in the active area to obtain a higher accuracy of the calculation results. The front DFB section and

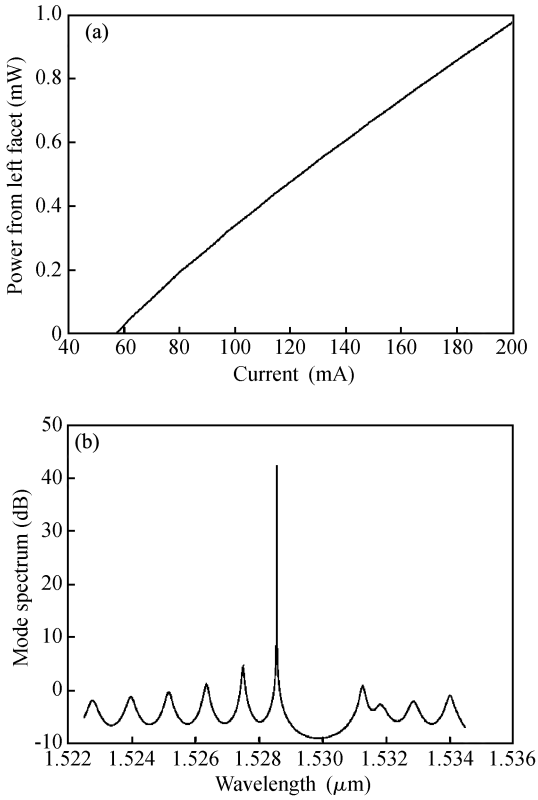

Fig. 4. Simulation results of (a) P–I curve and (b) spectrum of the rear DFB section.

the rear DFB section are simulated in sequence with the power reflectivity of the cleavage facet and the equivalent power reflectivity $R_{equr\text{-}21}$ or $R_{equf\text{-}21}$ obtained above.

Compared with the method of directly solving the lasing mode of the integrated device used before, this model is simpler and clearer in its physical mechanism, and is also more convenient because the computing time is much shorter. This model provides a new method for simulating the optical integrated device.

2.3. Simulation results

The P–I curves and the lasing spectra of the front DFB section and the rear DFB section are shown in Figs. 3 and 4 respectively. The lasing light of both sections emit from the left facet. The power of the rear DFB section is smaller because of absorption loss in the front section, and the threshold current is higher too. From the results shown in Figs. 3 and 4, the interaction between the two sections is small enough. Both DFB sections have a good side mode suppression ratio (SMSR) of about 40 dB. The simulation results prove that this monolithically integrated cascade device can provide two selectable wavelengths.

3. Device fabrication and measurements

A corresponding cascaded InP/InGaAsP DFB laser was fabricated. The material epitaxy and fabrication process have been reported in our previous work[7, 8]. The P–I curves of the front and rear DFB sections under continuous wave (CW) are shown in Fig. 5. The output power of the front DFB sec-

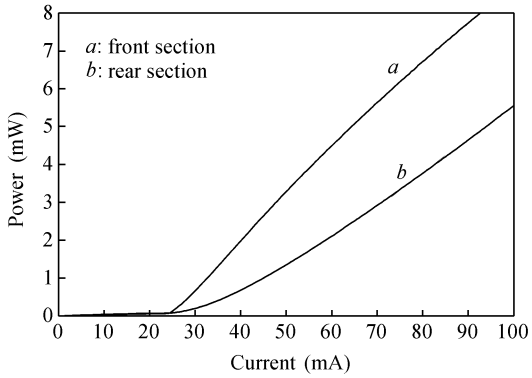

Fig. 5. P–I curve of the novel cascaded DFB lasers.

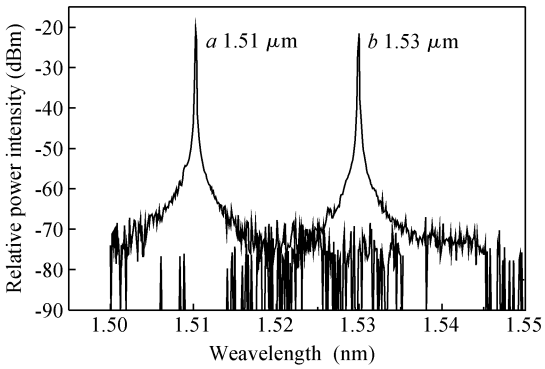

Fig. 6. Lasing spectra of the novel cascaded DFB lasers. a: Front section: 80 mA. b: Rear section: 80 mA.

tion achieves 10 mW at 100 mA and the output power of the rear DFB section achieves 5 mW at 100 mA. There is an apparent difference of output power between the simulation and the measurement result. We believe that it can be explained by following reasons. At first, in simulation just half the device is calculated considering the device structure symmetry, so the data of calculated output power should be doubled. Then, the active layer used in simulation is the ordinary multiple quantum wells with a bandgap wavelength of 1.55 μm, which causes a large deviation to both designed Bragg wavelengths of 1.51 μm and 1.53 μm. Therefore the calculated material gain of the active area is relatively small. Meanwhile, the active layer of the actual device is the asymmetric multiple quantum wells to achieve a flatter and wider material gain bandwidth than that of the ordinary quantum wells, which give the relatively larger material gain at the two selected Bragg wavelengths, hence the output power would be larger. Finally, when testing the rear section, the front section can amplify the light coming from the rear section like a semiconductor optical amplifier (SOA) because the front section is biased under its threshold current. The details can be found in our previous work[6]. The lasing spectra of both sections are shown in Fig. 6 respectively. Two different wavelengths, 1.51 μm and 1.53 μm (with a spacing of 20 nm), are obtained and the SMSR of the two wavelengths exceeds 40 dB.

4. Conclusion

A novel wavelength selectable cascaded DFB laser with two serial gratings is designed and simulated through TMM based on a new model. In simulation, the device is divided into two sections according its different Bragg grating periods and the transfer matrixes of each section are built. The equivalent reflectivity of each section is obtained from its respective transfer matrix. Each section is considered as a common DFB laser. The performance of each is simulated through self-consistently solving the gain equation, the coupled wave equation and the current continuity equation by the Newton iteration method. The boundary conditions of each section are based on the equivalent facet reflectivity achieved by TMM. The simulations are illustrated in detail and the results prove the feasibility of this kind of device. Finally, a cascaded DFB laser with two wavelengths is designed and fabricated with InP/InGaAsP quantum well structures. Two selectable wavelengths of 1.51 μm and 1.53 μm are realized in this monolithic integrated device and both SMSRs exceed 40 dB. So it can be used in a CWDM system as a light source.

Acknowledgement

The authors are grateful to the Multiple-function Optoelectronic Integration group, Institute of Semiconductors, CAS for device fabricating and testing.

References

[1] Winzer P J, Fidler F, Matthews M J, et al. 10-Gb/s upgrade of bidirectional CWDM systems using electronic equalization and FEC. J Lightwave Technol, 2003, 23(1): 203

[2] Ryu S W, Kim S B, Sim J S, et al. Asymmetric sampled grating diode for a multi-wavelength laser array. Optical Fiber Communication Conf, 2002, ThGG84: 730

[3] Young M G, Koren U, Miller B I, et al. Six wavelength laser array with integrated amplifier and modulator. Electron Lett, 1995, 31(21): 1835

[4] Pezeshki B, Mathur A, Zou S, et al. 12 nm tunable WDM source using an integrated laser array. Electron Lett, 2000, 36(9): 788

[5] Hong J, Kim H, Shepherd F, et al. Matrix-grating strongly gain-coupled (MG-SGC) DFB lasers with 34-nm continuous wavelength tuning range. IEEE Photonics Technol Lett, 1999, 11(5): 515

[6] Amann M C, Buus J. Tunable laser diodes. London: Artech House, 1988

[7] Xie Hongyun**,** Pan Jiaoqing, Zhao Lingjuan, et al. Dual-wavelength distributed feedback laser for CWDM based on non-identical quantum well. Chin Phys Lett, 2006, 23(1): 126

[8] Xie Hongyun, Zhou Fan, Wang Baojun, et al. Modified holographic exposure to fabricate varied Bragg grating in an identical chip. Chinese Journal of Semiconductors, 2005, 26(7): 160